Spin density and magnetism of rare-earth nickel borocarbides: $R\mathrm{Ni_2B_2C}$

Z. Zeng,* D. E. Ellis,† Diana Guenzburger, and E. Baggio-Saitovitch
Centro Brasileiro de Pesquisas Físicas, Rua Xavier Sigaud 150, 22290-180 Rio de Janeiro, RJ, Brazil
(Received 25 March 1996; revised manuscript received 30 July 1996)

The rare-earth spin moments in quarternary borocarbides $R\mathrm{Ni_2B_2C}$, R=Pr, Nd, Sm, Gd, Ho, Tm are determined by self-consistent density functional theory, using the embedded cluster formalism. Spin-polarized electronic structure calculations considering antiferromagnetic coupling between R-C layers are performed. Spin polarization of the lattice is examined in detail and related to observed ferromagnetic ordering in R-C layers and antiferromagnetic ordering between layers. The observed superconductivity of Y, Lu, Tm, Er, and Ho compounds and regions of coexistence with antiferromagnetism in Tm and Ho is discussed in terms of the magnitude of R moments, differences in R $4f$-$5d$ hybridization, and resulting lattice polarization. [S0163-1829(96)06642-8]

I. INTRODUCTION

For many years it was well understood that the presence of local moments in superconductors reduces the transition temperature T_c, either due to scattering mechanisms or due to spin-dependent exchange interactions between the moment and the electrons of the Cooper pairs. The discovery of ternary materials like $R\mathrm{Rh_4B_4}$ (R=rare earth) where superconductivity and magnetic order alternate or even coexist raised important questions about the details of the interactions and the possibility of coexistence of both types of long-range order. The observed coexistence of large magnetic moments and superconductivity in high-T_c materials was initially very surprising, and eventually rationalized in terms of spatial localization of moments, and their weak coupling to the superconducting fraction of the electron density.[1,2] Thus the recent synthesis of quarternary compounds such as $R\mathrm{Ni_2B_2C}$ ($6.2<T_c<16.6$ K) which clearly show the possibility of regions of coexistence and alternating order was especially significant.[3–7] In the present paper we consider in detail the nature of the spin distribution and spatial extent of polarization and the exchange field in the $R\mathrm{Ni_2B_2C}$ compounds with R=Pr, Nd, Sm, Gd, Ho, Tm.

First principles density functional theory is used within the embedded cluster formalism, using a nonrelativistic spin-polarized approach. Cluster analyses provide a view complementary to the band structure studies on these materials which have recently appeared;[8–11] here the localized orbital picture and a chemically intuitive description play a dominant role. An analysis of the effects of transition metal substitution, in compounds such as $\mathrm{Gd(Ni_{1-x}Co_x)B_2C}$, using the present variational linear combination of atomic orbitals (LCAO)-cluster formalism has been previously given.[12]

It has been useful to consider separately several different magnetic interactions responsible for pairbreaking in the superconducting state, as discussed, for example, in the review by Fischer.[1] These processes may be described most simply as (i) Spin-flip scattering of conduction electrons off magnetic ions (ii) Exchange interaction between localized moments and conduction electrons (iii) Polarization effects among the conduction electrons due to the exchange interaction.

These phenomena are inter-related, but to a great extent their effects are additive, with one or another process being dominant in a given material. The Heisenberg exchange Hamiltonian, H_{ex}, coupling the ion spin, S_i, to conduction electron spin, s,

$$H_{\mathrm{ex}}=I\sum_i S_i s \tag{1}$$

was used by Abrikosov and Gorkov (AG),[13] in the Green function approach, to successfully predict the reduction in T_c with magnetic impurity concentration x in alloys such as $\mathrm{La_{1-x}Gd_xAl_2}$.[14] Here the interaction parameter I can be positive or negative, denoting antiferromagnetic (AFM) or ferromagnetic (FM) coupling. It was noted quite early that the magnetic ordering temperature T_M and depression of superconductivity (SC) transition temperature T_c scales with the projection of the ion spin S upon the total moment J, thus identifying the dominant exchange mechanism. Specifically,

$$S_{\parallel}=\frac{(S\cdot J)}{(J\cdot J)}J=(g_J-1)J \tag{2}$$

with ion-ion interaction energies proportional to the de Gennes factor $(g_J-1)^2J(J+1)$.

Deviations from predicted behavior in materials such as $\mathrm{La_{1-x}Ce_xAl_2}$ (Ref. 15) and existence of reentrant superconductivity over a limited temperature range have been attributed to T-dependent scattering as described by the Kondo effect.[16] Extension of the AG theory by Fulde and Maki,[17] also by Decroux and Fischer[18] to multiple pair breaking mechanisms revealed the essentially additive nature of interactions (i)–(iii) listed above in reducing the critical magnetic field $H_{c2}(T)$. The possibility of coexistence of antiferromagnetic order and superconductivity was pointed out quite early by Baltensperger and Strässler.[19]

In order to describe polarization effects the effective exchange field H_I has typically been defined as

$$g_s\mu_B H_I=xI\langle S_z\rangle, \tag{3}$$

which can be seen as an average over Eq. (1) with $\langle S_z\rangle$ being the spatial average of the spin component parallel to the

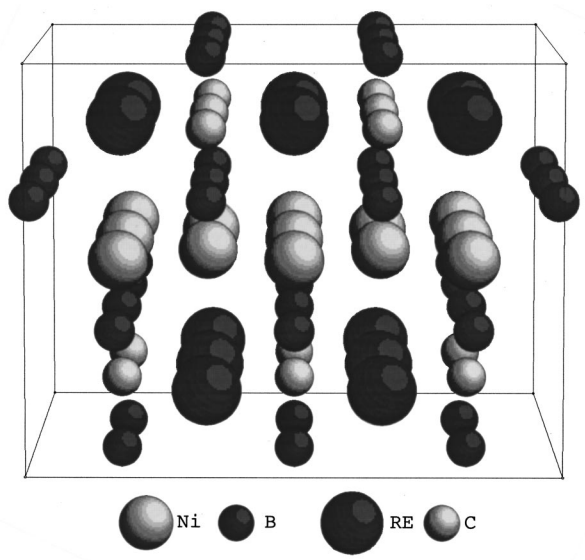

FIG. 1. Schematic of 73-atom $R_{12}Ni_{13}B_{36}C_{12}$ variational clusters.

quantization axis, and is thus proportional to the average magnetization $M(H,T)$. Here x represents the concentration of magnetic impurities. Fits to experiment show that the exchange field often dominates, being of the order of tens of Tesla, perhaps an order of magnitude larger than the direct magnetization, first considered by Ginzburg.[20] The reentrant rare-earth ternary compounds and their pseudoternary analogs display a wide range of magnetic order versus superconducting regions as a function of temperature. For example, $HoMo_6S_8$ shows evidence that superconductivity is destroyed by the internal field M due to ferromagnetic order, while exchange polarization is believed to be dominant in $ErRh_4B_4$.[1] The layer-structure R materials, such as RNi_2B_2C, reveal complex interactions and regions of coexistence between antiferromagnetic order and superconductivity whose properties have been studied by neutron diffraction,[21–23] NMR,[24–25] and as a function of pressure.[26–29] However, the presence or absence of superconductivity, the orientation and modulation of AFM coupling from one FM ordered R plane to another, the magnitudes and variation of ordering temperatures T_M and T_c remain to be explained. For example, despite the alternating layer structure of R-C planes and Ni-B slabs, the SC critical field is found to be highly isotropic, very unlike the high-T_c Cu-O based superconductors,[30–32] and in contrast to what may be expected of electrical conductivity.

The present work is aimed at obtaining an atomic-level understanding of the exchange field and magnetization, which have been treated before largely in the spatial average, or in the mean-field approximation. By examining the spatial variation of spin magnetization M_s and the first-principles exchange field H_x (defined below) we can show which is dominant in a given region of a complex material, and also understand the meaning of the spatial averages responsible for the exchange coupling parameter, I of Eqs. (1) and (3). In particular we will also see that the isotropic oscillatory Ruderman-Kittel-Kasuya-Yosida spatial variation of H_x, which follows for a uniform electron gas,[33] is not satisfied in

TABLE I. Self-consistent Mulliken atomic orbital populations and spin moments $2\langle S_z\rangle(\mu_B)$. The row $g_sS_\parallel$ is an estimate of the R^{+3} saturation spin moment parallel to J, from Ref. 53. $\langle M\rangle_{\rm para}$ is the experimental paramagnetic moment, which may be compared with the $4f$ only expected moment $\approx g_J\sqrt{J(J+1)}(\mu_B)$. $\langle M\rangle$ values for Pr, Nd, and Sm are for $PrNi_2Si_2$, $NdNi_2Si_2$, and $SmCo_2Ge_2$ from Ref. 54; values for Gd (Ref. 55), Ho, and Tm (Ref. 5) are for the RNi_2B_2C compounds.

	Pr		Nd		Sm		Gd		Ho		Tm	
	charge	spin	charge	spin	charge	spin	charge	spin	charge	spin	charge	spin
R $4f$	2.57	2.374	3.68	3.587	5.83	5.790	7.40	6.566	10.69	3.140	12.83	0.826
$5d$	0.34	0.029	0.30	0.036	0.24	0.042	0.47	0.091	0.22	0.023	0.18	0.004
$6s$	0.02	0.000	0.02	0.000	0.02	0.000	0.03	0.002	0.02	0.001	0.02	0.000
$6p$	0.05	−0.003	0.06	−0.004	0.06	−0.008	0.06	−0.007	0.05	−0.004	0.06	−0.001
net	2.30	2.400	2.21	3.619	2.09	5.828	2.26	6.652	2.08	3.160	2.09	0.829
Ni $3d$	9.10	0.000	9.10	0.000	9.09	0.000	9.13	0.000	9.09	0.000	9.08	0.000
$4s$	0.64	0.000	0.63	0.000	0.60	0.000	0.54	0.000	0.55	0.000	0.52	0.000
$4p$	0.52	0.000	0.52	0.000	0.52	0.000	0.51	0.001	0.56	0.000	0.56	0.000
net	−0.21	0.000	−0.20	0.000	−0.16	0.000	−0.12	0.001	−0.14	0.000	−0.10	0.000
B $2s$	1.24	0.000	1.24	0.001	1.25	0.001	1.29	0.001	1.26	0.000	1.26	0.000
$2p$	2.42	0.013	2.42	0.015	2.40	0.017	2.20	0.011	2.42	0.000	2.39	−0.002
net	−0.66	0.013	−0.67	0.016	−0.64	0.018	−0.50	0.012	−0.67	0.000	−0.65	−0.002
C $2s$	1.21	−0.001	1.22	−0.002	1.23	−0.002	1.22	−0.001	1.29	0.000	1.30	0.000
$2p$	4.24	−0.013	4.22	−0.016	4.20	−0.014	4.23	−0.005	4.21	0.008	4.18	0.003
net	−1.45	−0.014	−1.44	−0.018	−1.43	−0.016	−1.45	−0.006	−1.51	0.008	−1.48	0.003
$g_sS_\parallel$		−1.60		−2.46		−3.58		7.00		4.00		2.00
$g_J\sqrt{J(J+1)}$		3.58		3.62		0.85		7.94		10.60		7.56
$\langle M\rangle_{\rm expt}$		3.67		3.73		1.12		7.97		10.4		7.7

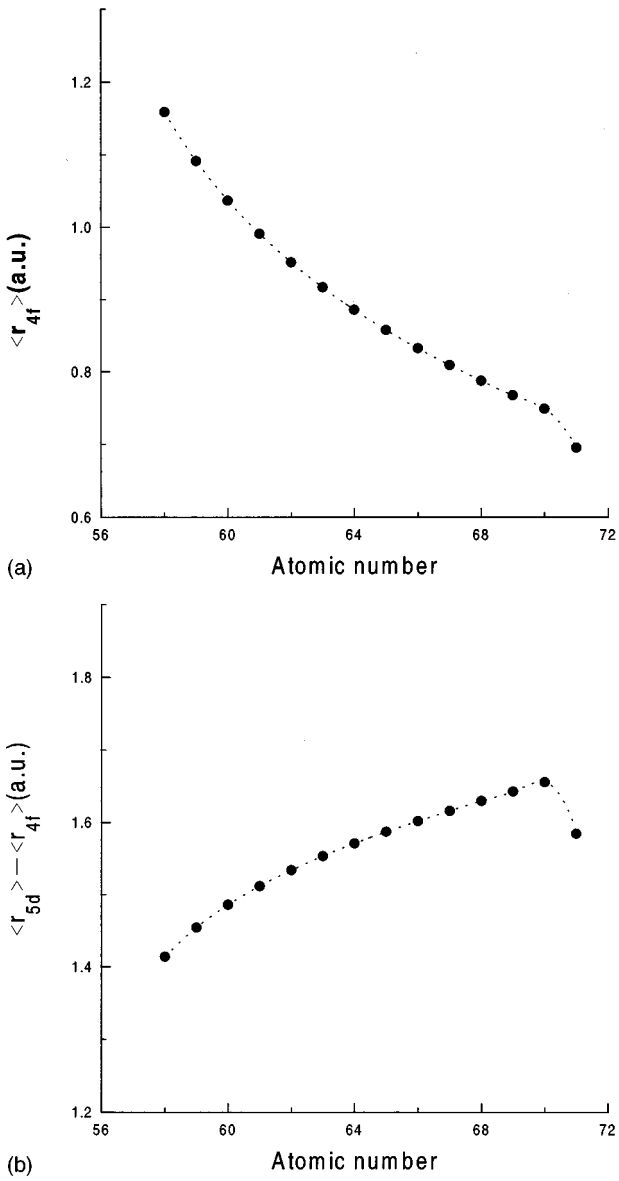

FIG. 2. Systematics of orbital radii in R^{3+} ions, according to nonrelativistic DF calculations; (a) Mean $4f$ radius $\langle r_{4f}\rangle$ and (b) Difference between $4f$ radius and mean $5d$ radius $\langle r_{5d}\rangle$.

more complex materials containing R, transition elements, and light elements displaying the full array of metallic, ionic, and covalent bonding.

It is generally assumed that pair-breaking fields seen by Cooper pairs result from spatial averages over regions of order of the SC coherence length ξ, which may be estimated to be of the order of 60–100 Å in the $R\mathrm{Ni}_2\mathrm{B}_2\mathrm{C}$ materials studied here.[34–35] However, this idea needs to be reconsidered in view of the intraplanar R-R distance of ~3.5 Å, interplanar distance of ~5.2 Å (corresponding R-R distance ~5.8 Å) and the resulting strong variation of magnetization and field throughout the solid, on a length scale of ~1 Å.

The spin magnetization may be defined as

$$M_s(\mathbf{r})=\frac{8\pi}{3}[\rho_\uparrow(\mathbf{r})-\rho_\downarrow(\mathbf{r})], \tag{4}$$

where ρ_σ are the up- and down-spin electron densities. M_S is directly accessible to experiment, for example by Mössbauer spectroscopic measurement of magnetic hyperfine fields at probe nuclei, as has been done for $(\mathrm{Ni}_{1-x}\mathrm{Fe}_x)$ substituted compounds.[37]

In density functional (DF) theory, the exchange field may be defined by

$$g_s\mu_B H_x(\mathbf{r})=V_{\mathrm{xc},\uparrow}(\mathbf{r})-V_{\mathrm{xc},\downarrow}(\mathbf{r}), \tag{5}$$

where $V_{\mathrm{XC},\sigma}$ are the exchange and correlation potentials for either spin.[38] In the standard nonrelativistic spin-polarized DF approach, the spin densities and potentials are determined by self-consistent iterations. That approach was followed in the present work, making use of the embedded cluster Discrete Variational method, which has been widely applied in metals, semiconductors, and ionic solids.[39]

Exchange and correlation potentials of varying levels of sophistication have been developed and used, in the present work the von Barth-Hedin form[40] has been employed. In the simplest Kohn-Sham approximation, that of the free-electron gas with exchange only,

$$g_s\mu_B H_x\cong(6/\pi)^{1/3}(\rho_\uparrow^{1/3}-\rho_\downarrow^{1/3}) \tag{6}$$

allowing some immediate qualitative deductions about the relative size of M_S and H_X. For example, M_S will dominate in the high spin-density region close to the magnetic ion, while H_X will dominate in the low-density exponential decay region and has a much longer range.

In the following, we give a quantitative analysis of spin magnetization and exchange field in the series $R\mathrm{Ni}_2\mathrm{B}_2\mathrm{C}$, with R=Pr, Nd, Sm, Gd, Ho, Tm. This analysis provides a possible explanation of the variation of strength in magnetic/SC coupling which is observed across the series. The remainder of the paper is organized as follows: In Sec. II we present details of the calculations, in Sec. III we present an analysis of resulting charge and spin densities. Our conclusions are given in Sec. IV.

II. DETAILS OF CALCULATIONS

The discrete variational (DV) embedded-cluster approach was used in the framework of first principles DF theory; as full details appear in the literature,[39] only a brief outline is given here. Effective atomic configurations of the cluster atoms were obtained self-consistently by iterating the charge and spin density in a nonrelativistic spin polarized approximation. It might be argued that relativistic effects are important, especially around the R site; however, the properties we seek to describe result primarily from polarization of the lighter atoms (Ni,B,C) and the essentially nonrelativistic valence electrons by the R spin moment. The effective exchange interaction between R ions, mediated by the lattice is found to be proportional to the spin component parallel to $J,S_\parallel$, as has been determined experimentally.[1,2,36] In fact, one result of considerable interest here is self-consistent determination of the $4f$-spin moment, or more precisely, its component $\langle S_Z\rangle$.

The variational clusters used consist of 73 atoms with composition $R_{12}\mathrm{Ni}_{13}\mathrm{B}_{36}\mathrm{C}_{12}$ as shown in Fig. 1. The embedding scheme treats interactions between the variational cluster and the infinitely extended host crystal, by constructing a

total charge (spin) density by superposition of cluster and host charge (spin) densities; i.e.

$$\rho_\sigma = \rho_{\sigma\text{cluster}} + \rho_{\sigma,\text{host}}. \tag{7}$$

A real-space sum of ~1400 external host atoms was sufficient to converge the short-range potential, while an Ewald procedure was used to sum the long-range Coulomb interactions. A double iteration scheme was carried out, by which both cluster and crystal are brought to self-consistency. Mulliken population analysis[41] of occupied cluster orbitals, which are expanded in a basis of numerical atomic orbitals (NAO), provides effective atomic configurations at each site, which are used to synthesize the host densities for subsequent iterations. The NAO basis is in turn constructed from the self-consistent cluster atomic configurations, in order to obtain a chemically intuitive view of the charge distribution. In the present work the basis included Ni $3spd$, $4sp$, B and C $2sp$, and R $4f$, $5spd$, $6sp$ functions in the valence space; inner shell orbitals were treated as a frozen core. Valence cluster symmetry orbitals were constructed as linear combinations of NAO which were explicitly orthogonalized against the core. The crystal structures and interatomic distances were taken from the literature.[42]

Symmetry constraints were applied to densities and Hamiltonian to achieve the desired AFM or FM order of alternating R-C planes. A three-dimensional numerical integration grid of ~45 000 points and several hundred self-consistent potential iterations was found adequate to determine densities of states (DOS), energy levels, charge distribution, and Mulliken spin and charge populations to the desired level of precision (<0.1 eV in energy, <0.001 e in charge/spin).

III. ELECTRONIC STRUCTURE AND MAGNETIC PROPERTIES

A. Charge distribution and bonding

The self-consistent charge populations and spin moments obtained by Mulliken population analysis are given in Table I. The general picture of bonding derived from Table I is of ionic interaction in the R-C planes and dominant covalent bonding between four-coordinated Ni and B in the Ni-B slabs. Instead of the formal trivalent charge state, we find R charge varying from 2.08–2.30 e and typical carbon charge of −1.45 e. Ni is seen to be nearly neutral, while B acts as an acceptor, with typical charge −0.6 e. Few details about charge distribution are given in published band calculations.[8–11] In an LMTO study on the related material YNi_2B_2C Lee *et al.* report net site populations for Ni of $s^{0.67}p^{0.87}d^{8.68}$ implying a net charge of −0.22, with net charges of +0.56 and +0.44 for B and C, respectively.[8] According to this calculation, the net charge on Y is −1.13. This large negative value is astonishing when we consider that Y has by far the lowest electronegativity of all four components. Our calculated value of +2.5 for YNi_2B_2C,[12] similar to the values encountered for the present compounds (Table I), seems more realistic. Part of this discrepancy may be ascribed to different manners of defining ''atomic charge'' in the two methods. Pellegrin *et al.* studied the Ni L_3 absorption edge of the pure metal and RNi_2B_2C (R=Y, Sm, Tb, Ho, Er, Tm, Lu) and concluded that Ni was near the $3d^9$ configuration in all compounds.[43] From the observed chemical shift of ~1 eV to higher energies for the Ni L_3 white line, they suggested a charge transfer from Ni to its B and C neighbors, presumably from the Ni $4s$ band. We suggest that the shift is indeed due to charging of B and C, but that the R is the donor. The experimental B K edge also gives evidence of strong hybridization between N $3d$ and B $2p$ states as found in both band structure calculations and the present cluster analyses.

The $4f$ occupancy is nonintegral, indicating hybridization with (primarily) R $5d$ orbitals.[44] A significant $5d$ occupancy on the R is observed, and accounts for the major part of the deviation from the nominal R^{+3} configuration, with $5d$ populations ranging from 0.18 (Tm) to 0.47 (Gd). The presence of f-d hybridization is crucial to an understanding of the magnetic polarization of the lattice, and is expected to diminish with the mean $4f$ radius $\langle r_{4f}\rangle$. The decrease in $\langle r_{4f}\rangle$ [Fig. 2(a)] and the more relevant essentially linear increase in $\langle r_{5d}\rangle - \langle r_{4f}\rangle$, shown in Fig. 2(b), give a simple explanation for the rapid reduction in coupling and hybridization between the corelike $4f$ and the rather diffuse $5d$ with increasing atomic number. Guo and Temerman have previously suggested strong f-d hybridization as the main factor in suppressing SC in $PrBa_2Cu_3O_{7-x}$, whereas all other $RBa_2Cu_3O_{7-x}$ 1-2-3 compounds exhibit high T_c.[45] As we will see, the strong overlap between R $5d$ and C $2p$ leads to extensive lattice polarization via the hybridization mechanism; the superexchange interaction between R in different lattice planes thus proceeds via a multilink process. Apparently the R $5d$-O $2p$ overlap in the 1-2-3 materials is considerably smaller than in RNi_2B_2C, as the observed magnetic ordering takes place at rather low temperatures, 2.3 K for Tb and <1 K for the other R.[46,47] The AFM ordering temperature T_M scales according to the de Gennes factor $S_\parallel(S_\parallel+1)$, (see Table II) again showing that the $S_\parallel$ spin exchange interaction is dominant.

The calculated $4f$ occupancy is fractionally larger than that of the nominal trivalent ion, ranging from 2.57 (Pr) to 12.83 (Tm). The excess $4f$ population may be attributed primarily to effects of hybridization with $5d$ orbitals. Concerning spin moments, we may compare our *antiferromagnetic* results (using magnetic structure found in experiment) for $GdNi_2B_2C$ with the *ferromagnetic* structure calculated by Coehoorn with the ASW method.[11] By artificially shifting the $4f$ minority spin levels to a large positive energy, he obtained a net spin on Gd of 7.27 μ_B, which corresponds to the full $4f^7$ subshell and some ferromagnetically coupled $5d$ contribution. He found induced moments of 0.03, 0.00, and −0.01 μ_B on Ni, B, and C respectively. Our fully variational antiferromagnetic results give 6.65 μ_B for the Gd moment, of which 0.09 μ_B is due to the $5d$ contribution. The moment on Ni is zero by symmetry, and small induced moments of 0.01 and −0.006 μ_B are predicted for B and C respectively.

Charge density contour maps are given in Fig. 3, showing the R-C plane, the Ni plane, and a plane containing Ni-B and B-C bonds in the Gd compound. Nearly circular contours and regions of low density between Gd and C characterize the ionic interaction, with Gd-C distance of 2.53 Å. The Ni-Ni distance of 2.53 Å, slightly less than that of metallic Ni, leads to typical metallic diffuse density in the Ni plane. The Ni-B bonds (2.13 Å) show considerable charge localiza-

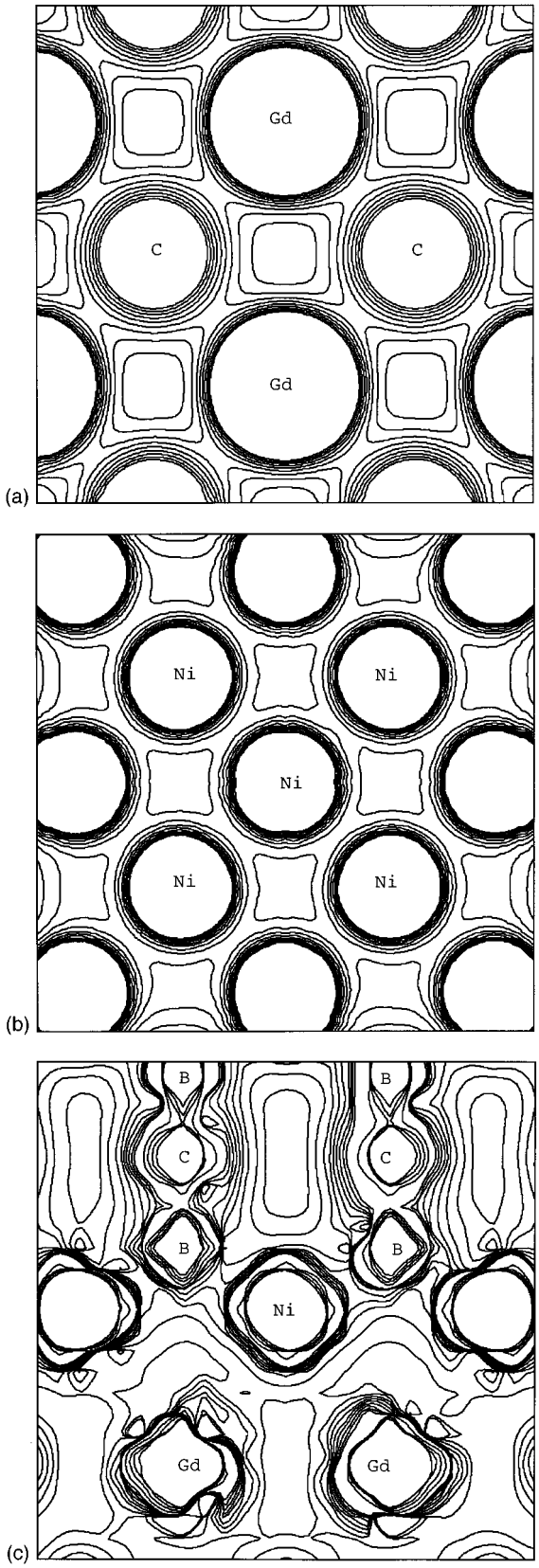

FIG. 3. Contour maps of self-consistent valence charge density in $GdNi_2B_2C$; contour interval is $10^{-2}\ e/a_0^3$. (a) Gd-C plane, (b) Ni plane, (c) Plane containing Ni-B and B-C bonds.

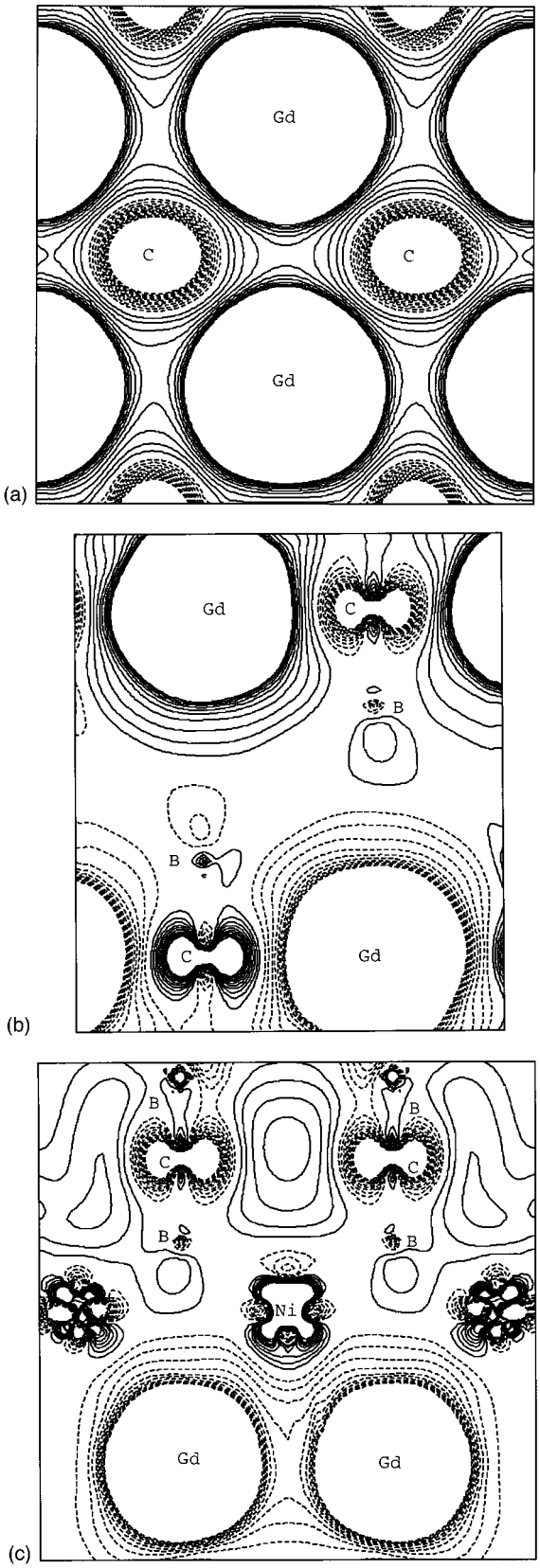

FIG. 4. Contour maps of self-consistent valence spin density in the antiferromagnetic state of $GdNi_2B_2C$; contour intervals of $10^{-4}\ e/a_0^3$. Solid curves represent positive values, dotted curves show negative values. (a) (001) Gd-C plane, containing spin up ions (b) (100) plane, containing spin up and spin down Gd ions. (c) Plane containing Ni, B, and C.

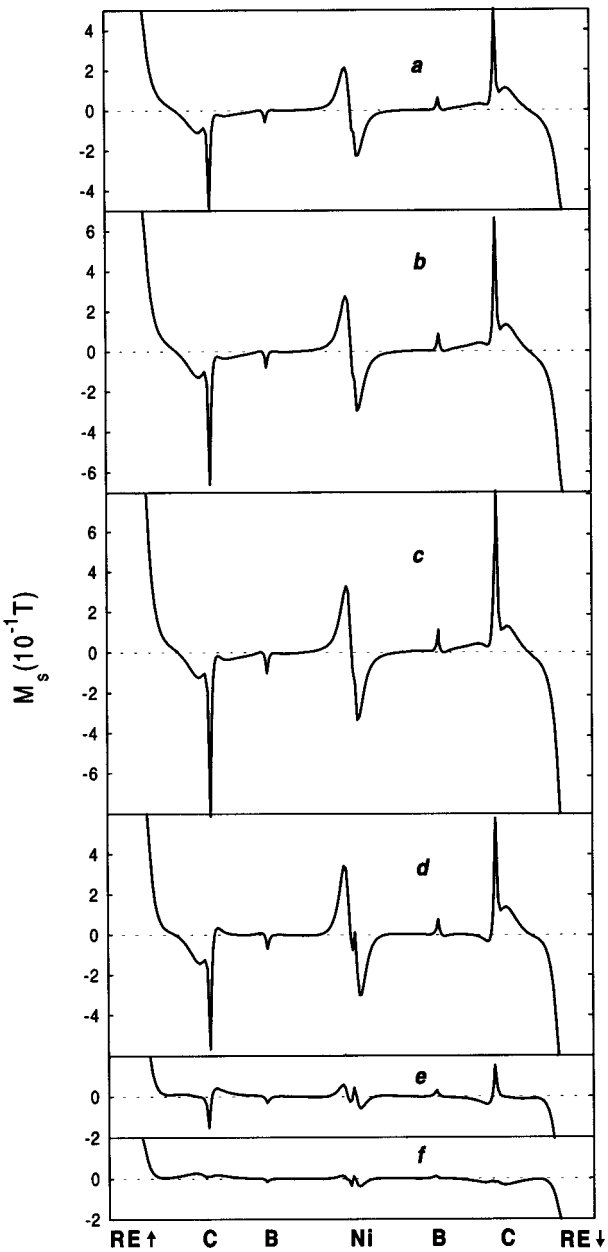

FIG. 5. Bond-line plots of valence spin magnetization M_S for antiferromagnetic states of $R\mathrm{Ni_2B_2C}$, beginning at one rare earth and passing from atom to atom along bond lines, terminating at a R in the next plane (distance $c/2$) above or below (After Ref. 49). (a) Pr, (b) Nd, (c) Sm, (d) Gd, (e) Ho, (f) Tm.

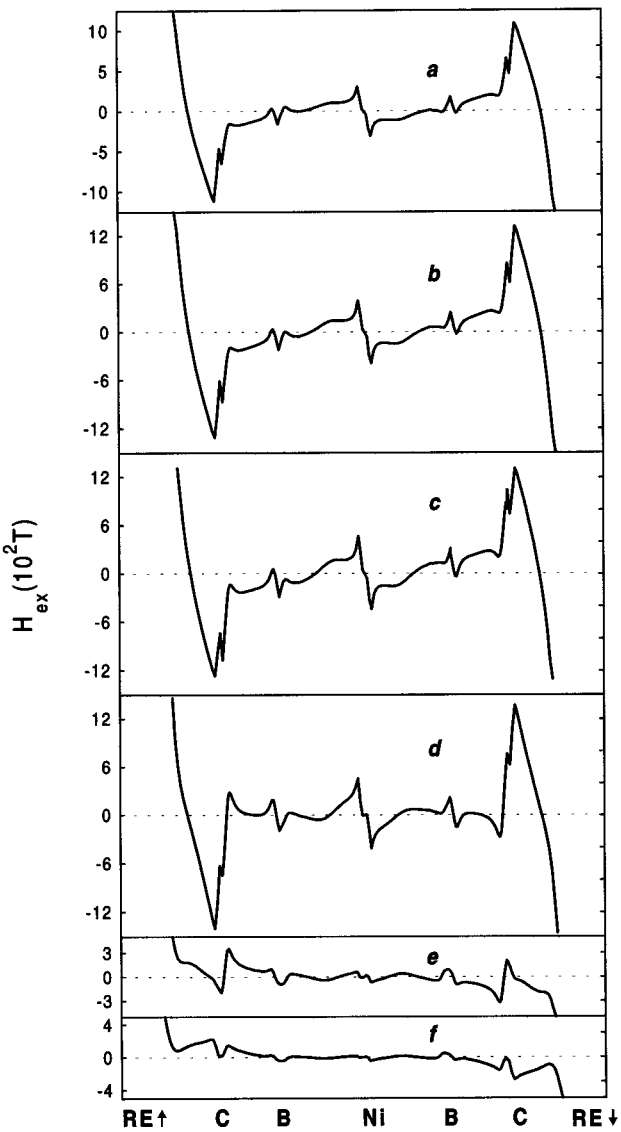

FIG. 6. Bond-line plots of net exchange field for antiferromagnetic states of $R\mathrm{Ni_2B_2C}$, beginning at one rare earth and passing from atom to atom along bond lines, terminating at a R in the next plane (distance $c/2$) above or below. (a) Pr, (b) Nd, (c) Sm, (d) Gd, (e) Ho, (f) Tm.

tion, and the strong B-C covalent bonds (1.43 Å) lead to a highly anisotropic local charge distribution; thus it is surprising that the critical field H_c appears to be essentially isotropic.[30–32] Electrical conductivity measurements on single crystals will help to clarify this point; to our knowledge such data are not yet available.

B. Spin moments and spin density

It is interesting that experimental magnetization generally suggests a R moment different from that of the bare trivalent ion, which has been attributed to crystal field splitting of the f level.[48] We suggest that in addition to temperature-dependent crystal field effects, $4f$-$5d$ hybridization may play an important part in determining the effective moment. Since the present calculations are nonrelativistic, we can not calculate directly the total moment arising from both spin and orbital components. However, as discussed in Sec. II, it is the effective spin moment parallel to **J** which is observed to control the exchange field, and indeed T_M of the $R\mathrm{Ni_2B_2C}$ compounds is found to correlate rather well with the de Gennes factor $(g_J-1)^2J(J+1)$, as does the reduction of T_c in the later R elements.[5,36] We can thus compare the expected saturation effective spin moment $g_sS_\parallel$ of the R^{+3} ion with the calculated $g_s\langle S_z\rangle$, and with experimental paramagnetic moments determined from susceptibilities $g_J\sqrt{J(J+1)}$, see Table I. The calculated $\langle S_z\rangle$ correlates approximately linearly with the absolute value of the free ion $S_\parallel$, with $\langle S_z\rangle$ exhibiting typically larger values for Pr, Nd,

TABLE II. Observed superconducting transition temperatures T_c(K), upper critical fields H_c(kG), and magnetic ordering temperatures T_m(K) for $R\mathrm{Ni_2B_2C}$.

R	T_c	H_c	T_m
Sm	none	none	9.9[g]
Gd	none	none	20[h]
Tb	none	none	15[h]
Dy	6.2[a]	?	10.3[a]
Ho	8.0[b]	4.5[i]	6[b]
	7.5[c]		8[c]
Er	10.5[d]	14.7[d]	5.9[d]
Tm	11[e]	21.2[g]	1.5[e]
Y	15.6[f]	32.0[h]	none
Lu	16.6[f]	?	none

[a]Reference 30.
[b]A. I. Goldman, C. Stassis, P. C. Canfield, J. Zarestky, P. Dervenagas, B. K. Cho, D. C. Johnston, and B. Sterlieb, Phys. Rev. B **50**, 9668 (1994).
[c]Reference 51.
[d]B. K. Cho, P. C. Canfield, L. L. Miller, D. C. Johnston, W. P. Beyermann, and A. Yatskar, Phys. Rev. B **52**, 3684 (1995).
[e]B. K. Cho, M. Xu, P. C. Canfield, L. L. Miller, and D. C. Johnston, Phys. Rev. B **52**, 12 852 (1995).
[f]Reference 42(a).
[g]Reference 42(b).
[h]Reference 30.
[i]Reference 5.
[g]B. K. Cho, Ming Xu, P. C. Canfield, L. L. Miller, and D. C. Johnston, Phys. Rev. B **52**, 3676 (1995).
[h]Reference 34.

and Sm, as would be expected. However, values of $\langle S_z \rangle$ are systematically smaller than $S_\parallel$ for the latter part of the R series; i.e., Gd, Ho, and Tm.

Contour maps of calculated spin density, proportional to the spin-magnetization density M_s of Eq. 4 are presented in Fig. 4 for the AFM state of $\mathrm{GdNi_2B_2C}$. Values are shown for one Gd-C plane, for a plane containing both spin up and spin down Gd ions, and for a plane containing Ni, B, and C. The spin coupling between R and its nearest neighbor C shows an interesting variation across the R series studied here. For the lighter R, the more extended $5d$ leads to a *negative* polarization of the region around C, i.e., an antiferromagnetic coupling. With contraction of R $5d$, some positive features begin to appear in ρ_s for Gd, which grow in intensity for Ho, and finally appear as a fully *positive* polarization around C in the Tm compound; i.e., a ferromagnetic coupling.

To understand the nature of long-range spin polarization via the exchange interaction, we consider the magnetization density M_s along bond lines. A previous study has been made of M_s in Ref. 49, where we demonstrated the crucial role of R $4f$-$5d$ hybridization in transmitting spin polarization to the lattice. Thus, beginning at one R, we follow a zig-zag path along bonds from one atom to another, finally terminating at another R in a plane at a distance $c/2$ above or below the starting point. Valence contributions to M_s are shown for each of the cases studied in Fig. 5 (reproduced from Ref. 49). The large $4f$ polarization is essentially off scale, while the (FM coupled) R $5d$ density is clearly visible along with its polarization of the C near neighbor via $5d$-C $2p$ mixing. A small polarization wave on the magnetically hard B site is followed by a relatively large response of the paramagnetic Ni atom. Due to the AFM symmetry, the *net* polarization of Ni must be zero; however, local spin density values above/below the symmetry plane amount to as much as 0.006 $e/a_0{}^3$ which corresponds to a local magnetic field of 0.34 T in the maximum-moment case of Gd.

TABLE III. Exchange energy differences ΔV_x (meV) and corresponding exchange field H_x(T) calculated along Ni-B bond lines. Both peak values and root-mean-square values are given.

	Pr	Nd	Sm	Gd	Ho	Tm
$\Delta V_{\max}$	35	45	54	53	6.7	1.8
ΔV_{rms}	12	15	19	16	4.3	1.6
$H_{x,\max}$	302	390	466	457	58	15
$H_{x,\mathrm{rms}}$	100	130	161	137	37	13

As discussed in Sec. I, the exchange field H_x due to differences in spin up and spin down potential is frequently considered to be the dominant factor in superconductor pair-breaking. This field is obtained directly in our self-consistent DF calculations, as given by Eq. (5), and is presented along bond lines in Fig. 6. As expected from the previous discussion H_x is qualitatively similar to M_s; however, H_x is of longer range and thus dominates at large distances from the driving moment, or in regions of low spin density. Peak and root-mean-square (rms) values of difference in exchange-correlation potential $\Delta V_{\mathrm{xc}} = V_{\mathrm{xc},\uparrow} - V_{\mathrm{xc},\downarrow}$ and the corresponding fields H_x, calculated along the Ni-B bond line, are given in Table III. The rms exchange energies, which range from 1.6 (Tm) to 19 (Sm) meV can be compared in magnitude with a superconducting energy gap of $\Delta = 5.3$ meV found for $\mathrm{YNi_2B_2C}$[50] and the pair-breaking energy 2Δ. As seen in Fig. 6 and Table III, peak values of H_x as large as $\sim$450 T are found in the interatomic regions surrounding Ni and C, and thus are much larger than typical SC critical fields H_c of 4–5 T in these materials. It is thus very interesting to see how spatial averaging over the extent ($\sim\xi$) of SC wave functions permits the coexistence of superconductivity with such large local fields. It is also notable that a rotation of only 12° in orientation of moment in adjacent planes of the AFM structure of Ho is sufficient to provide a net field capable of suppressing superconductivity.[51] The existence of compositional disorder between B and C sites, and possible C vacancies inferred from recent Mössbauer studies[11] provides another important mechanism for disrupting the average cancellation of positive and negative regions of H_x.

Magnetic dipolar fields H_D arising on the rare earths are also sometimes mentioned as possible contributors to pair breaking. Electronic shielding effects make it difficult to give quantitative values for the dipolar fields, which are certainly much smaller than those due to exchange, but may be of similar magnitude to the local spin magnetization. To obtain some upper-bound estimates of H_D, we carried out classical point-dipolar lattice sums for typical values of R moments, evaluating the (unshielded) values of H_D throughout the crystal. Due to the D_{2d} crystal symmetry, H_D does *not* vanish at the $z=0$ Ni plane, and values of 2–4 T are found in the vicinity of the Ni site. Thus a quantitative treatment of all

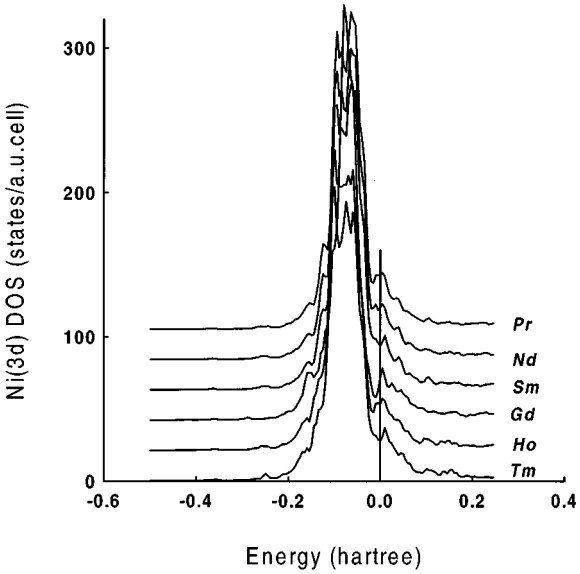

FIG. 7. Partial densities of states for Ni $3d$ in $R\mathrm{Ni}_2\mathrm{B}_2\mathrm{C}$. Parent compound is indicated in the legend. Successive curves have been offset by $x,2x,3x,\ldots,x=21$ for ease of viewing.

pair-breaking contributions will require consideration of direct and shielding contributions to H_D.

C. Densities of states

Densities of states were generated by broadening discrete cluster energy levels with a Lorentzian line shape of width 0.14 eV for comparison with band structure models and eventual spectroscopic data. Partial densities of states (PDOS) which resolve local atomic structure and orbital composition were generated by weighting cluster energy levels by appropriate Mulliken populations in the usual fashion.[39] Consistent with published band structures,[8–11] we find a highly structured and broad valence band, with the Fermi energy E_F falling on or near a secondary peak dominated by Ni and B character, in all the compounds studied.

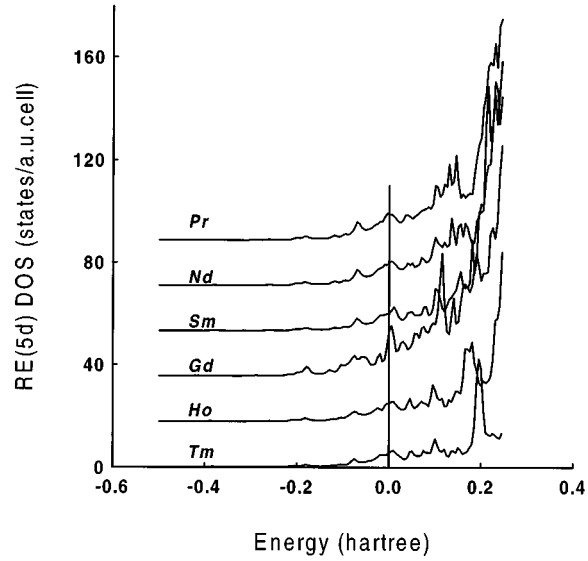

FIG. 9. Partial densities of states for R $5d$. Successive curves have been offset by $x,2x,3x,\ldots,x=18$ for ease of viewing.

Interpretation of ground-state DOS requires care, since it is well known that final state relaxation, correlation effects, and fundamental limitations of (ground state) DF theory all apply to description of excited state phenomena. For example, with a partially filled R $4f^n$ shell, one will expect to find (and does find) a narrow $4f$ band straddling E_F. However, Coulomb repulsion and other correlation effects of several eV in magnitude cause large shifts of the final state energy upon addition/subtraction of an electron from the highly localized $4f$ shell. Nevertheless, the *ground-state* description of level position and occupancy remains highly useful; and examination of PDOS composition permits prediction of some excitation properties. The calculated ex-

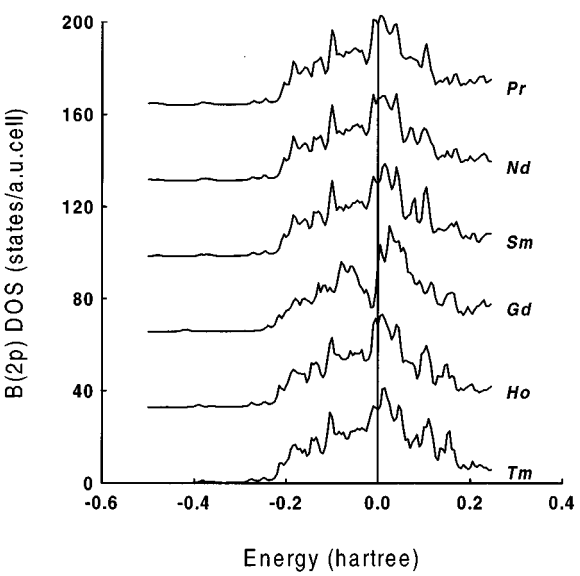

FIG. 8. Partial densities of states for B $2p$. Successive curves have been offset by $x,2x,3x,\ldots,x=33$ for ease of viewing.

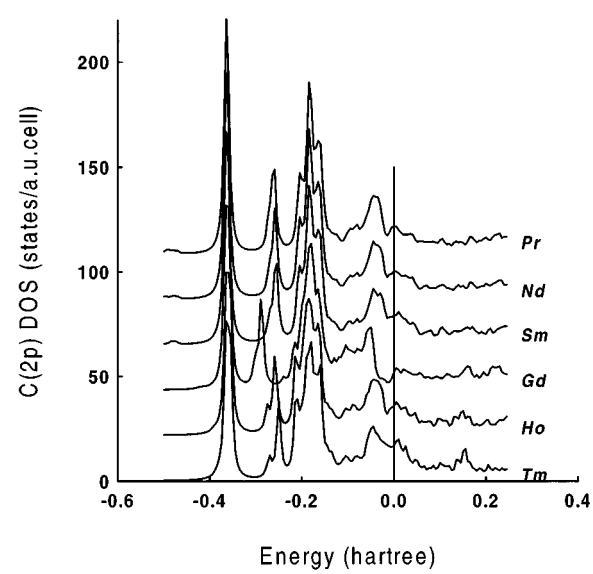

FIG. 10. Partial densities of states for C $2p$. Successive curves have been offset by $x,2x,3x,\ldots,x=22$.

TABLE IV. Calculated R $4f$ exchange splitting Δ_{4f} (eV) in $R\mathrm{Ni_2B_2C}$ and proportionality factors Δ_{4f}/M_z and Δ_{4f}/M_f (units of eV/μ_B). $M_z=g_s\langle S_z\rangle$ is net spin moment of R and $M_f=g_s\langle S_{4f}\rangle$ is net spin moment of $4f$ shell.

	Pr	Nd	Sm	Gd	Ho	Tm
Δ_{4f}	1.56	2.38	4.05	4.97	2.38	0.68
Δ_{4f}/M_z	0.65	0.66	0.69	0.75	0.75	0.82
Δ_{4f}/M_f	0.66	0.66	0.70	0.76	0.76	0.82

change splitting Δ_{4f} of the $4f_\uparrow$-$4f_\downarrow$ bands is given in Table IV along with the factors $A_{\mathrm{total}}=\Delta_{4f}/g_s\langle S_z\rangle$ and $A_{4f}=\Delta_{4f}/g_s\langle S_{4f}\rangle$ which give the (average) proportionality between the exchange field and the local R spin-moment. With constant $\langle r_{4f}\rangle$, one would expect A_{total} also to be constant; however, A_{total} is seen to increase slowly across the R series, which can be understood in terms of the increasing $4f$ spin density due to contraction of the $4f$ shell with increasing Z. We also see that $A_{\mathrm{total}}\cong A_{4f}$, verifying the dominance of the $4f$ driving moment and relatively small screening effects of the $5d$ shell and polarized neighbors.

It is appropriate to examine PDOS of Ni, B, C, and R valence levels to ascertain structure around E_F which is important for low-lying excitations, conductivity, and formation of the SC state. The relative size of PDOS for $E\sim E_F$ gives a clue as to the critical wave function composition: for example in $\mathrm{NdNi_2B_2C}$ we find Ni $3d$ (18.3)>B $2p$ (17.6)>C $2p$ (3.4)>Nd $5d$ (2.3) in units of states/(Hartree-cell), with negligible components of other states. [Again, we note that the R $4f$ contribution can only be ''counted'' in ground state properties; $4f$ excitation will greatly shift the corresponding $4f$ PDOS. Thus, the $4f$ contribution to DOS(E_F) was not included in the above numbers, nor in the DOS diagrams.] While quantitative differences are noted, qualitative similarities are seen in all the R cases studied. The Ni $3d$, B $2p$, C $2p$, and R $5d$ PDOS are given in Figs. 7–10; these data are most relevant when we take a real-space view of the conductivity processes. We see that the B $2p$ PDOS structure is of major importance in forming the c-direction conductive pathway, and also take note of the suggestion of Mattheiss[9] that the stiff Ni-B bond with its high-frequency vibrational structure may be a key to understanding the relatively high-T_c values. The observed ^{10}B, ^{11}B isotope effect on T_c is an important further indication of the ''normal'' electron-phonon mechanism and of the role played by B in SC pair formation.[52]

IV. CONCLUDING REMARKS

We have reported spin-polarized Density Functional embedded cluster studies of the quarternary compounds R $\mathrm{Ni_2B_2C}$, with R=Pr, Nd, Sm, Gd, Ho, and Tm. The R $4f$ spin moments were determined self-consistently and found to correlate reasonably well with experimentally determined R^{3+} spin-component moments $S_\parallel$. Ferromagnetic coupling of R $5d$ to $4f$ electrons provides the pathway for long-range interaction of the f moment with atoms at a distance of several coordination shells. Resulting spin polarization of the lattice was calculated; magnetization and exchange fields were mapped and discussed in terms of observed antiferromagnetic order, reentrant superconductivity, and coexistence of SC and AFM order. Local exchange fields as large as 450 T are predicted; we thus obtain some information about the local structure underlying the relatively long-range volume averaging over field ''seen'' by SC pairs, which permits coexistence of SC and magnetic order. Ni $3d$ and B $2p$ states in the vicinity of E_F were found to be dominant in conductivity properties in all compounds studied. Lesser C $2p$ and R $5d$ contributions to the partial densities of states provide essential components for the observed (and still surprising) isotropic SC critical fields. Thus, single crystal measurements of anisotropy of electrical conductivity would be very useful.

ACKNOWLEDGMENTS

This work was supported by the $\mathrm{CNP_q}$, under the project RHAE-New Materials Project No. 610195/92-1 and by the U.S. National Science Foundation, through the Materials Research Center at Northwestern University, Grant No. DMR-9120521. Calculations were carried out at the Cray YMP computer facility of the Universidade Federal do Rio Grande do Sul.

*On leave from the Institute of Solid-State Physics, Academica Sinica, Hefei 230031, People's Republic of China.

†Dept. of Physics and Astronomy and Materials Research Center, Northwestern University, Evanston, IL, 60208.

[1] O. Fischer, in *Ferromagnetic Materials*, edited by K. H. J. Buschow and E. P. Wohlfarth (North-Holland, Amsterdam, 1990), Vol. 5, p. 465.

[2] *Theories of High Temperature Superconductivity*, edited by J. W. Halley (Addison-Wesley, New York, 1988); M. B. Maple, in *Magnetism*, edited by H. Suhl (Academic, New York, 1973), Vol. 5, p. 289; R. J. Elliot, in *Magnetic Properties of Rare Earth Metals*, edited by R. J. Elliot (Plenum, London, 1972), p. 1; P. G. De Gennes, C. R. Acad. Sci. **247**, 1836 (1966); J. Phys. Radium **23**, 510 (1962).

[3] R. J. Cava, H. Takagi, B. Batlogg, H. W. Zandbergen, J. J. Krajewski, W. F. Peck, Jr., R. B. van Dover, R. J. Felder, T. Siegrist, K. Mizuhashi, J. O. Lee, H. Eisake, S. A. Carter, and S. Uchida, Nature **367**, 146 (1994).

[4] R. Nagarajan, C. Mazumdar, Z. Hossain, S. K. Dhar, K. V. Gopalakrishnan, L. C. Gupta, C. Godart, B. D. Padalia, and R. Vijayaraghaven, Phys. Rev. Lett. **72**, 274 (1994).

[5] H. Eisaki, H. Takagi, R. J. Cava, B. Batlogg, J. J. Krajewski, W. F. Peck, K. Mizuhashi, J. O. Lee, and S. Uchida, Phys. Rev. B **50**, 647 (1994).

[6] Y. Y. Sun, I. Rusakova, R. L. Meng, Y. Cao, P. Gautier-Picard, and D. W. Chu, Physica C **230**, 435 (1994).

[7] L. C. Gupta, R. Nagarajan, C. Godart, S. K. Dhar, C. Mazumdar, Z. Hossain, C. Levy-Clement, B. D. Padalia, and R. Vijayaraghavan, Physica C **235–240**, 150 (1994).

[8] J. I. Lee, T. S. Zhao, I. G. Kim, B. I. Min, and S. J. Youn, Phys. Rev. B **50**, 4030 (1994).

[9] L. F. Mattheiss, T. Siegrist, and R. J. Cava, Solid State Commun. **91**, 587 (1994); L. F. Mattheiss, Phys. Rev. B **49**, 13 279 (1994).

[10] W. E. Pickett and D. J. Singh, Phys. Rev. Lett. **72**, 3702 (1994);

J. Y. Rhee, X. Wang, and B. N. Harmon, Phys. Rev. B **51**, 15 585 (1995).

[11] R. Coehoorn, Physica C **228**, 331 (1994); F. M. Mulder, J. H. V. J. Brabers, R. Coehoorn, R. C. Thiel, K. H. J. Buschow, and F. R. de Boer, J. Alloys Compds. **217**, 118 (1995).

[12] Z. Zeng, D. Guenzburger, D. E. Ellis, and E. M. Baggio-Saitovitch, Phys. Rev. B **53**, 6613 (1996).

[13] A. A. Abrikosov and L. P. Gorkov, JETP **12**, 1243 (1961).

[14] M. B. Maple, Phys. Lett. A **26**, 513 (1968).

[15] G. Riblet and K. Winzer, Solid State Commun. **9**, 1663 (1971).

[16] E. Müller-Hartmann and J. Zittarz, Phys. Rev. Lett. **26**, 428 (1971).

[17] P. Fulde and K. Maki, Phys. Rev. **141**, 275 (1966).

[18] M. Decroux and O. Fischer, in *Superconductivity in Ternary Compounds* II, Vol. 34 of *Topics in Current Physics*, edited by M. B. Maple and O. Fischer (Springer, Berlin, 1982), p. 57.

[19] W. Baltensperger and S. Strässler, Phys. Kondens. Mater. **1**, 20 (1963).

[20] V. L. Ginzburg, JETP **4**, 153 (1957).

[21] Q. Huang, A. Santoro, T. E. Grigereit, J. W. Lynn, R. J. Cava, J. J. Krajewski, and W. F. Peck, Jr., Phys. Rev. B **51**, 3701 (1995).

[22] S. K. Sinha, J. W. Lynn, T. E. Grigereit, Z. Hossain, L. C. Gupta, R. Nagarajan, and C. Godart, Phys. Rev. B **51**, 681 (1995).

[23] J. Zarestky, C. Stassis, A. I. Goldman, P. C. Canfield, D. Dervenagas, B. K. Cho, and D. C. Johnston, Phys. Rev. B **51**, 678 (1995).

[24] M. E. Hanson, F. Lefloch, W. H. Hong, W. G. Clark, M. D. Lan, C. C. Hoellwarth, P. Klavins, and R. N. Shelton, Phys. Rev. B **51**, 674 (1995).

[25] T. Kohara, T. Oda, K. Ueda, Y. Yamada, A. Majahan, K. Elankumaran, Z. Hossian, L. C. Gupta, R. Nagarajan, R. Nijayaraghavan, and C. Mazumdar, Phys. Rev. B **51**, 3985 (1995).

[26] H. Schmidt and H. F. Braun, Physica C **229**, 315 (1994).

[27] C. Murayama, N. Mori, H. Takagi, H. Eisaki, K. Mizuhashi, S. Uchida, and R. J. Cava, Physica C **235–240**, 2545 (1994).

[28] E. Alleno, J. J. Neumeier, J. D. Thompson, P. C. Canfield, and B. K. Cho, Physica C **242**, 169 (1995).

[29] S. A. Carter, B. Batlogg, R. J. Cava, J. J. Krajewski, and W. F. Peck, Jr., Phys. Rev. B **51**, 12 644 (1995).

[30] B. K. Cho, P. C. Canfield, and D. C. Johnston, Phys. Rev. B **52**, 3844 (1995).

[31] M. Xu, B. K. Cho, P. C. Canfield, D. K. Finnemore, D. C. Johnston, and D. E. Farrell, Physica C **235–240**, 2533 (1994).

[32] E. Johnston-Halperin, J. Fiedler, D. E. Farrell, M. Xu, B. K. Cho, P. C. Canfield, D. K. Finnemore, and D. C. Johnston, Phys. Rev. B **51**, 12 852 (1995).

[33] C. Kittel, in *Solid State Physics*, edited by F. Seitz, D. Turnbull, and H. Ehrenreich (Academic, New York, 1968) Vol. 22, p. 1.

[34] M. Xu, P. C. Canfield, J. E. Ostenson, D. K. Finnemore, B. K. Cho, Z. R. Wang, and D. C. Johnston, Physica C **227**, 321 (1994).

[35] F. Canepa, P. Manfrinetti, A. Palenzona, M. R. Cimberle, E. Giannini, D. Marre and M. Putti, Nuovo Cimento **16**, 1857 (1994).

[36] J. El Massalami, S. L. Bud'ko, B. Giordanengo, E. M. Baggio-Saitovitch, Physica C **244**, 41 (1995).

[37] D. R. Sanchez, H. Micklitz, M. B. Fontes, S. L. Bud'ko, and E. Baggio-Saitovitch, Phys. Rev. Lett. **76**, 507 (1996); S. L. Bud'ko, M. B. Fontes, D. Aliaga-Guerra, and E. M. B. Saitovitch, Phys. Rev. B **52**, 305 (1995).

[38] J. C. Slater, *Quantum Theory of Molecules and Solids* (McGraw-Hill, New York, 1974), Vol. 4; R. G. Parr and W.-T. Yang, *Density-Functional Theory of Atoms and Molecules* (Oxford University Press, Oxford, 1989).

[39] D. E. Ellis and J. Guo, in *Electronic Density Functional Theory of Molecules, Clusters, and Solids*, edited by D. E. Ellis (Kluwer, Dordrecht, 1994) p. 263; B. Delley and D. E. Ellis, J. Chem. Phys. **76**, 1949 (1982); D. E. Ellis, G. A. Benesh and E. Byrom, Phys. Rev. B **20**, 1198 (1979); A. Rosen, D. E. Ellis, H. Adachi, and F. W. Averill, J. Chem. Phys. **65**, 3629 (1976); E. J. Baerends, D. E. Ellis, and P. Ros, Chem. Phys. **2**, 41 (1973); D. E. Ellis and G. S. Painter, Phys. Rev. B **2**, 2887 (1970).

[40] U. Von Barth and L. Hedin, J. Phys. C **5**, 129 (1972).

[41] R. Mulliken J. Chem. Phys. **23**, 1833 (1955).

[42] (a) R. J. Cava, H. Takagi, H. W. Zandbergen, J. J. Krawjewski, W. F. Peck, Jr., T. Siegrist, B. Batlogg, R. B. vanDover, R. J. Felder, K. Mizuhasi, J. O. Lee, H. Eisaki, and S. Uchida, Nature **367**, 252 (1994); (b) K. Prassides, A. Lappas, M. Buchgeister and P. Verges, Europhys. Lett. **29**, 641 (1995); (c) T. Siegrist, H. W. Zandbergen, R. J. Cava, J. J. Krajewski, and W. F. Peck, Jr., Nature **367**, 254 (1994).

[43] E. Pellegrin, C. T. Chen, G. Meigs, R. J. Cava, J. J. Krajewski, and W. F. Peck, Jr., Phys. Rev. B **51**, 16 159 (1995).

[44] An additional factor contributing to nonintegral $4f$ occupation is our use of thermal broadening of the Fermi-Dirac occupation numbers, with DE=0.01 a.u. to smooth and accelerate the self-consistent iterations. This effect is small in comparison to $4f$-valence electron hybridization

[45] G. Y. Guo and W. M. Temerman, Phys. Rev. B **41**, 6372 (1990).

[46] M. B. Maple, Y. Dalichaouch, J. M. Ferreira, R. R. Hake, B. W. Lee, J. J. Neumeier, M. S. Torkachvilli, K. N. Yang, H. Zhou, R. P. Guertin and M. V. Kuric, Physica B **148**, 155 (1987), and references therein.

[47] M. B. Maple, J. M. Ferreira, R. R. Hake, B. W. Lee, J. J. Neumeier, C. L. Seaman, K. N. Yang, and H. Zhou, J. Less-Common Met. **149**, 405 (1989).

[48] B. D. Dunlap, J. Magn, Magn. Mater. **37**, 211 (1983); B. D. Dunlap, L. N. Hall, F. Behroozi, G. W. Crabtree, and D. G. Niarchos, Phys. Rev. B **39**, 6224 (1988); H. Zhou, S. E. Lambert, M. B. Maple, S. K. Malik, and B. D. Dunlap, *ibid.* **36**, 594 (1987).

[49] Z. Zeng, D. Guenzburger, D. E. Ellis, and E. M. B. Saitovitch, Physica C (to be published).

[50] T. Ekino, H. Fujii, M. Kosugi, Y. Zenitani, and J. Akimitsu, Physica C **235–240**, 2529 (1994).

[51] T. E. Grigereit, J. W. Lynn, Q. Huang, A. Santoro, R. J. Cava, J. J. Krajewski, and W. F. Peck, Phys. Rev. Lett. **73**, 2756 (1994).

[52] D. D. Lawrie and J. P. Franck, Physica C **245**, 159 (1995).

[53] S. Legvold, in *Ferromagnetic Materials*, edited by E. P. Wohlfarth (North-Holland, Amsterdam, 1980) Vol. 1, p. 183.

[54] A. Szytula and J. Leciejewicz, *Handbook of Crystal Structures and Magnetic Properties of Rare Earth Intermetallics* (CRC, Boca Raton, 1994).

[55] M. El Massalami, B. Giordanengo, J. Mondragon, E. M. Baggio-Saitovitch, A. Takeuchi, J. Voiron, and A. Sulpice, J. Phys. Condens. Matt. **7**, 10 015 (1995).